Biosensors and Bioelectronics 25 (2010) 2603–2610

Contents lists available at ScienceDirect

Biosensors and Bioelectronics

journal homepage: www.elsevier.com/locate/bios

Construction of optical glucose nanobiosensor with high sensitivity and selectivity at physiological pH on the basis of organic–inorganic hybrid microgels

Weitai Wu, Ting Zhou, Michael Aiello, Shuiqin Zhou*

Department of Chemistry and The Center for Engineered Polymeric Materials, College of Staten Island, and The Graduate Center, The City University of New York, Staten Island, NY 10314, United States

ARTICLE INFO

Article history:
Received 5 March 2010
Received in revised form 15 April 2010
Accepted 19 April 2010
Available online 28 April 2010

Keywords:
Glucose nanobiosensor
Fluorescence
Quantum dots
Microgels
Organic–inorganic hybrids

ABSTRACT

A new class of optical glucose nanobiosensors with high sensitivity and selectivity at physiological pH is described. To construct these glucose nanobiosensors, the fluorescent CdS quantum dots (QDs), serving as the optical code, were incorporated into the glucose-sensitive poly(*N*-isopropylacrylamide-acrylamide-2-acrylamidomethyl-5-fluorophenylboronic acid) copolymer microgels, via both in situ growth method and "breathing in" method, respectively. The polymeric gel can adapt to surrounding glucose concentrations, and regulate the fluorescence of the embedded QDs, converting biochemical signals into optical signals. The gradual swelling of the gel would lead to the quenching of the fluorescence at the elevated glucose concentrations. The hybrid microgels displayed high selectivity to glucose over the potential primary interferents of lactate and human serum albumin in the physiologically important glucose concentration range. The stability, reversibility, and sensitivity of the organic–inorganic hybrid microgel-based biosensors were also systematically studied. These general properties of our nanobiosensors are well tunable under appropriate tailor on the hybrid microgels, in particular, simply through the change in the crosslinking degree of the microgels. The optical glucose nanobiosensors based on the organic–inorganic hybrid microgels have shown the potential for a third generation fluorescent biosensor.

1. Introduction

The development of active nanostructures, capable of performing a function or executing a specific task, is currently a major focus of research efforts in bio-/nanotechnology. One already highly successful nanodevice paradigm is the nanosensor: a designed nanostructure, which, when addressed optically, can provide information about its local environment through its optical response (Bardelang et al., 2008; Li et al., 2009; Lim et al., 2009; Zhang et al., 2004). There is an urgent need to develop sensor for continuous *in vivo* glucose monitoring at physiological pH in subjects with diabetes mellitus (Pickup et al., 2005), which represents one of the largest health concerns of the 21st century with worldwide prevalence (King et al., 1998). There is also a critical need for monitoring glucose levels in nondiabetic acute care patients, since large variations in blood glucose level have been observed in nondiabetic patients as a common consequence of surgery or acute illness (Matz et al., 2006; McCowen et al., 2001). Therefore, developing a sensor for reliable, relatively non-invasive, and continuous glucose monitoring would result in markedly improved outcomes for patients with diabetes and patients who experience acute care induced hyperglycemia (Schmeltz et al., 2007; Van den Berghe et al., 2006).

The majority of current glucose measurement methods utilize the enzyme glucose oxidase. However, enzyme based systems suffer from instabilities due to denaturation, difficulties associated with sterilization, and cost when used in a format suitable for continuous sensing (Pickup et al., 2005). This has led to considerable research interest in developing synthetic ligands for binding and detecting glucose. The best ligands identified for binding glucose in aqueous media are boronic acids (Davis and Wareham, 1999). These boronic acid-based ligands have been coupled with polymer (Alexeev et al., 2003; Kabilan et al., 2005; Lee et al., 2004; Liu et al., 2009; Muscatello et al., 2009; Shoji and Freund, 2002; Suri et al., 2003; Tierney et al., 2009; Yang et al., 2006, 2008) for continuous glucose sensing. For example, holographic sensors based on the phenylboronic acid (PBA) copolymer film have been developed by Lowe's group (Lee et al., 2004; Yang et al., 2006, 2008), while Asher's group developed photonic crystal glucose sensing systems based on the PBA-modified hydrogels (Alexeev et al., 2003; Muscatello et al., 2009). While these glucose sensors exploited a change in diffraction or reflection, an alternative approach that records a change in fluorescence has been reported. Fluorescence measurements cause little or no damage to the host system. With the appropriate choice of optical labels, molecules can in theory be excited and the emission interrogated from outside the body

* Corresponding author. Tel.: +1 718 982 3897; fax: +1 718 982 3910.
E-mail address: shuiqin.zhou@csi.cuny.edu (S. Zhou).

0956-5663/$ – see front matter © 2010 Elsevier B.V. All rights reserved.
doi:10.1016/j.bios.2010.04.030

(Pickup et al., 2005), thus providing the potential for completely non-invasive sensing. Different fluorescent organic moieties have been coupled with the boronic acid-based ligands (Peng and Qin, 2008; Yang et al., 2001). On the other hand, there is a growing interest in using quantum dots (QDs) as optical labels for biosensing events due to their size-controlled fluorescence properties, high quantum yield, and stability against photobleaching over organic fluorophores (Bardelang et al., 2008). Techniques include measuring the changes in fluorescence resonance energy transfer (FRET) between a fluorescent donor and an acceptor because of competitive displacement (Cordes et al., 2006; Freeman et al., 2009; Tang et al., 2008), as well as the glucose-induced changes in intrinsic fluorescence of H_2O_2-sensitive QDs (Gill et al., 2008). However, these systems are only good for homogeneous detection. Recently, we have found that the fluorescence of CdS QDs immobilized in the microgels containing 3-aminophenyl boronic acid could be quenched when the microgels swelled at the elevated glucose concentration (Wu et al., 2009a). While this discovery validated a novel starting point for constructing glucose sensors, many problems, such as stability, sensitivity, reversibility, and selectivity, remain unexplored. In particular, this sensor could only sense glucose at alkaline pH (~8.8) but not at lower pH values, while the working of a glucose sensor at physiological pH and even acidic conditions (diabetic ketoacidosis) is vital for development of practical sensors (Vantyghem et al., 1999). Giving the fact that the organic–inorganic hybrid microgels have some special advantages for *in vivo* sensing, such as a tunable size from submicrons to tens of nanometers, large surface area for bioconjugation, potential biocompatibility, interior network structure for the incorporation of therapeutics, and a very short response time (Reese et al., 2004; Zhang et al., 2004; Zhang et al., 2007), knowing how to utilize different routes in an orthogonal fashion to obtain novel glucose sensors that can work at physiological pH is one of the key requirements for future development in this area.

In this paper, we design a class of optical glucose nanobiosensors that response at physiological pH by utilizing a new boronate derivative, the poly(*N*-isopropylacrylamide-acrylamide-2-acrylamidomethyl-5-fluorophenylboronic acid) [p(NIPAM–AAm–FPBA)] microgel network chains (Supplementary, Scheme S-1), as glucose recognition element. The glucose reporter ligand of 2-acrylamidomethyl-5-fluorophenylboronic acid possess not only a lower pK_a due to the presence of electron-withdrawing fluorine group (Kabilan et al., 2005), but also the diminished interference due to the selective binding of the 2-acrylamidophenylboronate derivative to glucose over lactate (Yang et al., 2006). The fluorescent CdS QDs serving as optical code were immobilized into the microgels via both in situ growth method and "breathing in" method, respectively. The in situ method is to transform the pre-loaded Cd^{2+} ions to CdS QDs directly in the interior of the microgel template, while the "breathing in" method is to load the pre-synthesized CdS QDs into the microgel template. The structure stability, reversibility, sensitivity, and potential molecular interferences from lactate, a key metabolite in blood (Burtis and Ashwood, 1999), and human serum albumin (HSA) of these glucose nanobiosensors were systematically investigated. The sensitivity of the sensor to glucose can be tuned by a simple adjustment of the crosslinking degree of the microgels. In addition, the synthetic methods presented here provide us a feasibility to control the distribution of QDs in the interior of the microgels and thus their biocompatibility (Wu et al., 2009b), as well as to replace the model CdS QDs by other QDs if necessary. The beauty of this class of systems, which differentiates it from other examples of glucose sensors, is the easy functionalization and the potential for the combination of a number of different functions, such as glucose detection and self-regulated insulin delivery, into a single nano-object that can work at physiological conditions. These hybrid microgel-based optical glucose "meters" with tunable sensitivity, high selectivity, stable structure, and excellent reversibility are likely to be highly useful for research, diagnosis, and monitoring.

2. Experimental

2.1. Materials

D(+)-Glucose and 2-aminomethyl-5-fluorophenylboronic acid (FPBA) were purchased from ACROS and Combi-Blocks Inc., respectively. All other chemicals were purchased from Aldrich. NIPAM was recrystallized from a 1:1 hexane–acetone mixture and dried in vacuum. Acrylic acid (AA) was purified by distillation under reduced pressure. $Cd(ClO_4)_2{\cdot}H_2O$, mercaptosuccinic acid (MSA), thioacetamide, AAm, *N*,*N*′-methylenebisacrylamide (MBAAm), ammonium persulfate (APS), sodium dodecyl sulfate (SDS), sodium L-lactate, HSA, and *N*-(3-dimethylaminopropyl)-*N*′-ethyl-carbodiimide hydrochloride (EDC) were used as received without further purification.

2.2. Synthesis of the glucose-sensitive p(NIPAM–AAm–FPBA)–CdS hybrid microgels

2.2.1. Synthesis of p(NIPAM–AAm–FPBA) microgels

The p(NIPAM–AAm–AA) microgels with 7.0 mol% of AAm, 7.1 mol% of AA, and 4.3 mol% of MBAAm were prepared by free radical precipitation copolymerization and purified using the procedure as described before (Wu et al., 2009a). The FPBA-functionalized p(NIPAM–AAm–FPBA) microgels were then synthesized via the EDC catalyzed coupling of FPBA to COOH groups in AA units. First, 0.255 g of FPBA and 0.231 g of EDC were dissolved in 35 mL of water. The solution was cooled in an ice bath, and then 20 mL of purified p(NIPAM–AAm–AA) microgels was added. The reaction was allowed to proceed for 4 h in ice water bath. The resultant products were purified by dialysis against very frequently changed water for at least 1 week.

2.2.2. In situ synthesis of CdS QDs in p(NIPAM–AAm–FPBA) microgels (in situ method)

The mixture of 0.1431 g $Cd(ClO_4)_2{\cdot}H_2O$ with 20 mL p(NIPAM–AAm–FPBA) microgel dispersions was stirred at room temperature for 1 day under a N_2 purge. After that, excess Cd^{2+} ions were removed by centrifugation (20,000 rpm, 10 min), decantation, and dialysis against water for 2 days. The purified microgels loaded with Cd^{2+} ions were heated to 60 °C under a N_2 purge. After 30 min, 5 mL thioacetamide solution (0.0146 g/mL) was added dropwise. The temperature was raised to 85 °C and the color gradually turned to brilliant yellow. The mixture was further stirred for 1 h under N_2 atmosphere. The resulted microgels incorporated with in situ grown CdS QDs were then purified by centrifugation, decantation, and dialysis against very frequently changed water for 3 days and coded as p(NIPAM–AAm–FPBA)–CdS_{is}.

2.2.3. Pre-synthesis of CdS QDs and their upload into p(NIPAM–AAm–FPBA) microgels ("breathing in" method)

5.2 nm CdS QDs were pre-synthesized using MSA as a capping agent. Typically, a mixture of 0.0475 g $Cd(ClO_4)_2{\cdot}H_2O$, 0.1201 g MSA, and water (30 mL) was heated to 35 °C under a N_2 purge. After 30 min, 5 mL thioacetamide solution (0.0146 g/mL) was dropwisely added. The temperature was raised to 100 °C, and the color gradually turned to brilliant yellow. The mixture was further stirred for 1 h under N_2 atmosphere. The resulted MSA-capped CdS QDs were then purified by repeated centrifugation, decantation, and redispersed in water. To load the CdS QDs into microgels, 30 mL of purified p(NIPAM–AAm–FPBA) microgels were kept in an ice

water bath for 30 min, and then 20 mL of MSA-capped CdS QDs was added. The mixture was kept in ice water bath for 1 day. The resultant hybrid microgels loaded with the MSA-capped CdS QDs were purified by dialysis against very frequently changed water for at least 1 week and coded as p(NIPAM–AAm–FPBA)–CdS_{ab}.

2.3. Characterization

The UV–vis absorption spectra were obtained on a Thermo Electron Co. Helios β UV–vis Spectroscopy. The PL spectra were obtained on a JOBIN YVON Co. FluoroMax®-3 Spectrofluorometer. The transmission electron microscopy (TEM) images were taken on a FEI TECNAI transmission electron microscope at an accelerating voltage of 120 kV. The hydrodynamic radius (R_h) was determined on a standard laser light scattering spectrometer (BI-200SM) equipped with a BI-9000 AT digital time correlator and a He–Ne laser (35 mW, 633 nm) as the light source.

3. Results and discussion

3.1. Synthesis of the glucose-sensitive hybrid microgels

Generally, our strategy to prepare the hybrid microgels for glucose probing involves the first synthesis of a glucose-sensitive microgels p(NIPAM–AAm–FPBA) possessing desired functional groups (Scheme S-1), followed by the incorporation of CdS QDs into the template microgels. The FPBA groups are in equilibrium between the undissociated (uncharged) and the dissociated (charged) forms in aqueous solution (Scheme S-2) (Davis and Wareham, 1999; Kabilan et al., 2005). Both forms react reversibly with 1,2-*cis*-diols such as glucose. The complexation of the uncharged form with glucose is unstable because it is highly susceptible to hydrolysis, but the binding with glucose causes the thermodynamically more favorable charged form. Our previous work has shown that microgels fabricated with 3-PBA are responsive to glucose at pH ≈ 8.8 (Wu et al., 2009a), but they plummet precipitously in glucose sensitivity at pH < 8.0 (Sartain et al., 2008). FPBA is more hydrophilic than 3-PBA due to its polar character (Kabilan et al., 2005). The electron-withdrawing fluoric group should also cause a decreased electron density on the boron atom, making the FPBA stronger in acidity with a lower pK_a. Thus, the FPBA-modified microgels should exhibit glucose sensitivity at a physiological pH. Fig. 1A shows the R_h values of the p(NIPAM–AAm–FPBA) microgels as a function of glucose concentration, measured in a 5.0 mM phosphate buffer solution (PBS) of pH 7.38 at 22.1 °C. The binding of glucose increases the degree of ionization on the p(NIPAM–AAm–FPBA) microgels and builds up a

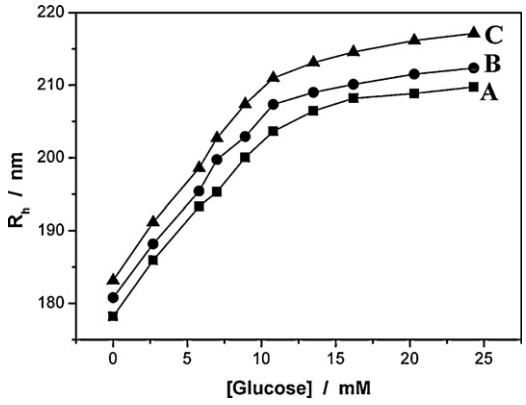

Fig. 1. Average R_h value of the p(NIPAM–AAm–FPBA) (A) template microgels, and p(NIPAM–AAm–FPBA)–CdS_{is} (B) and p(NIPAM–AAm–FPBA)–CdS_{ab} hybrid microgels (C), as a function of glucose concentration, measured at pH 7.38 and T = 22.1 °C.

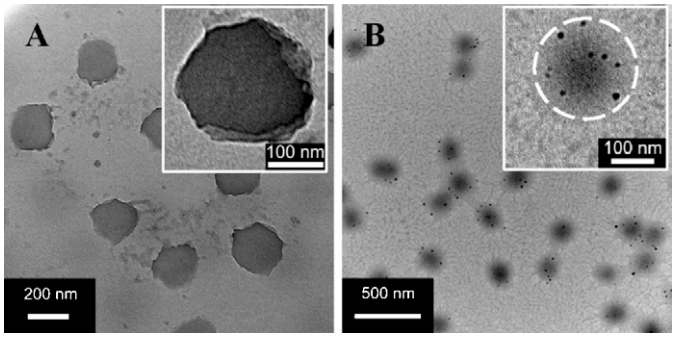

Fig. 2. Typical TEM images of (A) p(NIPAM–AAm–FPBA)–CdS_{is} and (B) p(NIPAM–AAm–FPBA)–CdS_{ab} hybrid microgels.

Donnan potential for the microgels to swell. The R_h of the microgel particles increases with the increase in glucose concentration. The glucose-induced swelling curve flats off when the glucose concentration is above 16.2 mM where the microgel network chains stretch to nearly a maximum. This result indicates that the FPBA functionalized microgels do demonstrate glucose sensitivity at the physiological pH.

Both amino groups and charged boronate groups are able to link CdS QDs (Xiong et al., 2007), allowing the introduction of optical code into the microgels. Herein, we have chosen pH ≈ 5.9, corresponding to the nearly fully uncharged state of FPBA groups, for uptake and immobilization of CdS QDs inside the p(NIPAM–AAm–FPBA) microgels. Our motivation is to use the $-NH_2$ groups in the AAm units to anchor the CdS QDs and also to protect these QDs from agglomeration or release. The hybrid microgels incorporated with CdS QDs are still glucose-sensitive at physiological pH, but become larger in size in comparison with their template microgels (Fig. 1B and C). This could be related to the relatively compact structure of the p(NIPAM–AAm–FPBA) template microgels due to the hydrophobic FPBA groups and high crosslinking density (4.3 mol%). The embedded CdS QDs filled into the relatively compact chain networks, and thus expanded the total volume of the microgels. Fig. 2 shows the TEM images of the p(NIPAM–AAm–FPBA)–CdS_{is} (A) and p(NIPAM–AAm–FPBA)–CdS_{ab} (B) hybrid microgels prepared from in situ growth method and "breathing in" method, respectively. For in situ growth method, the small precursor Cd^{2+} ions could diffuse to any location of the template microgels to access the $-NH_2$ ligands that are randomly distributed on the polymer network chains, thus the in situ formed CdS QDs (higher contrast) are randomly distributed nearly everywhere through the whole volume of microgel particles. In contrast, the pre-synthesized QDs (~5.2 nm) could only diffuse into the relatively large pore area of the template microgels. Therefore, the p(NIPAM–AAm–FPBA)–CdS_{ab} hybrid microgels display a plum-pudding like structure interspersed with many discrete dark spots of CdS QDs. Importantly, both hybrid microgel were very stable in water. The hydrophilic pAAm segments prevented the hybrid microgels from aggregation in PBS for several months at room temperature.

3.2. PL properties of the glucose-sensitive hybrid microgels

The CdS QDs exhibit extremely strong quantum confinement in the hybrid microgels to produce photoluminescence (PL) emissions (Fig. S-2). The glucose-induced volume phase transition of the hybrid microgels could significantly affect the PL properties of the CdS QDs embedded in the interior of the microgels. Fig. 3A and B show the glucose-induced evolution of PL emissions centered at 603 nm and 606 nm for p(NIPAM–AAm–FPBA)–CdS_{is} and p(NIPAM–AAm–FPBA)–CdS_{ab} hybrid microgels, respectively, at pH

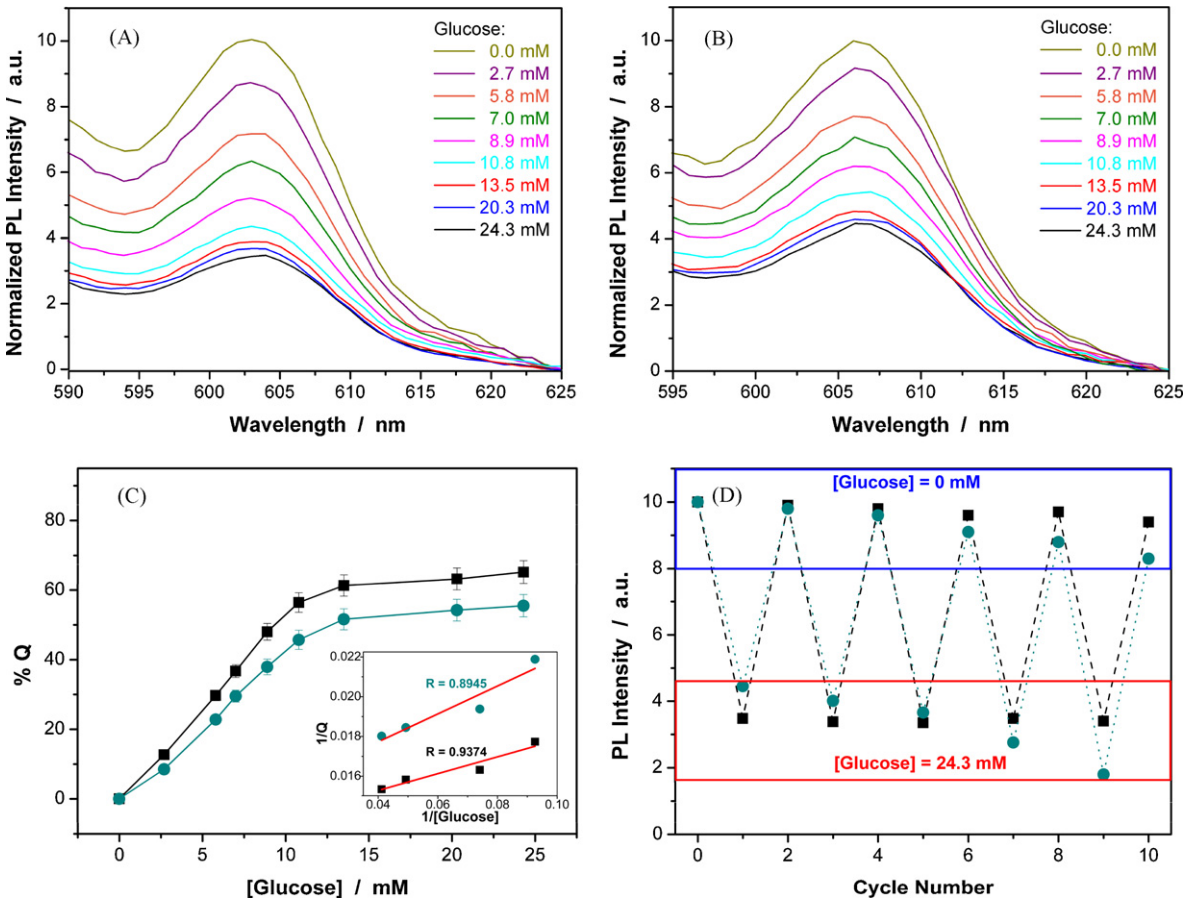

Fig. 3. (A and B) Normalized PL spectra and (C) quenched PL as a function of glucose concentration in PBS at pH 7.38 for p(NIPAM–AAm–FPBA)–CdS_{is} hybrid microgels at 603 nm (A, ■), and p(NIPAM–AAm–FPBA)–CdS_{ab} hybrid microgels at 606 nm (B, ●). Linear plot in inset of (C) showing the glucose-responsive PL properties in the reciprocal space, with [glucose] = 10.8–24.3 mM. (D) PL quenching and recovery cycles upon the repeated addition (24.3 mM) and dialysis removal of glucose (0 mM) in the dispersion medium of the corresponding hybrid microgels. The excitation wavelength was 390 nm.

7.38. It is interesting that the two types of hybrid microgels behave the same trend in response to a glucose concentration change. The PL of CdS QDs was gradually quenched when the microgels gradually swelled up with additions of D-glucose. Fig. 3C summarizes the glucose sensitivity based on the fluorescence quenching of the CdS QDs embedded in the hybrid microgels. The fluorescence quenching of the CdS QDs can reach as high as 65% and 56% for the p(NIPAM–AAm–FPBA)–CdS_{is} and p(NIPAM–AAm–FPBA)–CdS_{ab} hybrid microgels, respectively. The comparison of Fig. 1 with Fig. 3C indicates that the change in the PL intensity of the QDs embedded in the microgels conspicuously fits with the size change of the hybrid microgels. The PL quenching of the QDs almost linearly increased with the glucose concentration from 0 to 10.8 mM with a detection limit about 0.5 mM, and then slowed down at higher glucose concentrations when the microgel network chains stretched to near a maximum. However, the quenching effect is not saturated when the glucose concentration is above 10.8 mM. For the glucose concentration range from 10.8 to 24.3 mM, the linear plot in the reciprocal space (inset of Fig. 3C) clearly displays the glucose-responsive PL properties in a more orthogonal fashion. It should be mentioned that glucose by itself in the tested concentration range of 0–25 mM has no effect on the fluorescence of the surfactant-stabilized CdS (Wu et al., 2009a) and CdSe/ZnS QDs (Gill et al., 2008). The Fasting Plasma Glucose (FPG) test is the most commonly used test for diabetes mellitus. According to the standards of American Diabetes Association, normal fasting blood glucose is below 5.5 mM (100 mg/dL). A person with a fasting blood glucose level between 5.5 mM and 6.9 mM (100 and 125 mg/dL) belongs to pre-diabetes. If the blood glucose level rises to 7.0 mM (126 mg/dL) or above, a person has diabetes. It is clear that our hybrid microgel systems exhibit high sensitivity to the typical glucose concentrations across the physiologically important glucose level.

Two factors should be considered to explain how the glucose-induced swelling of the microgels could trigger the fluorescence quenching. One is related to the change in the refractive index of the microgel during its swelling/deswelling, which results in the change in the Rayleigh scattering, as well as the local refractive index around the CdS QDs (Mulvaney, 1996). We believe that the increase in the number of emission quenching centers located on the polymer–CdS QDs interface provides the second scenario for the PL quenching during the microgel swelling. At low glucose concentrations, the contract polymer chain networks have less elastic tension. In the swollen states at higher glucose concentrations, the polymer chains tend to dissolve, however, the crosslinkage of the polymer chains hinders the network expansion, creating elastic tensions localized at the crosslinking points. Because of the binding between the polymer ligands and the CdS QDs, the CdS QDs also act as crosslinking points, introducing an elastic tension in the bond that could stretch the polymer–CdS QDs interface, creating interfacial states that quench the PL (Scheme S-2). Similar phenomenon has been reported by Wuister's group (Wuister et al., 2004) that the short stabilizer molecules (2-mercaptoethanolamine) can propagate the exogenous strain to the CdTe QDs surface, creating surface quenching states. Since the reversible PL quenching/recovery of the QDs embedded in the interior of the microgels are caused from the glucose-induced volume phase transitions of the template micro-

gels, the kinetics of the glucose-induced PL quenching/recovery will depend on the swelling/shrinking kinetics of the microgels in response to a glucose concentration change. It is well known that the rate of the stimuli-induced volume change of a hydrogel particle is scaled as l^{-2}, where l is the relevant length scale of gel particle (Li and Tanaka, 1990). Indeed, nanosecond to microsecond (e.g., ~100 ns) volume phase transitions have been determined for individual poly(*N*-isopropylacrylamide) microgel particles in the size range of ~200–350 nm (Reese et al., 2004; Wang et al., 2001). We expect that the kinetics of the glucose-induced volume change and PL quenching/recovery of our hybrid microgel-based glucose sensors (R_h ~ 180–210 nm) should be in the hundreds nanosecond scale.

The reaction of glucose with boronic acids is unique since the covalent bonds formed between the boronic acid and *cis*-diols are reversible (Davis and Wareham, 1999; Lee et al., 2004; Zhang et al., 2007). As glucose is removed from the bathing medium of hybrid microgels by dialysis against very frequently changed water, the content of boronate anions in the gel phase is decreased and the microgel network chains contract. Fig. 3D shows the PL quenching and recovery cycles of the p(NIPAM–AAm–FPBA)–CdS_{is} and p(NIPAM–AAm–FPBA)–CdS_{ab} hybrid microgels, respectively, upon the repeated addition and dialysis removal of glucose in the dispersion medium up to five swelling/deswelling cycles. Addition of glucose (24.3 mM) can swell the get network, inducing a dramatic quenching of PL intensity. When the glucose was removed through dialysis, the hybrid microgels shrank in size, which induce the recovery of PL intensity. For p(NIPAM–AAm–FPBA)–CdS_{ab} hybrid microgels, a gradual decrease in PL intensity occurred after repeated cycles of addition and dialysis removal of glucose. This phenomenon is likely due to the escape of the QDs from the host microgels during the repeated swelling/deswelling process upon the change of glucose concentration. The repeating cycles of addition and dialysis removal of glucose against very frequently changed water will also remove those free CdS QDs escaped from the interior of hybrid microgels in the bathing medium. In such a situation, the amount of CdS QDs remained in the interior of the hybrid microgels will gradually decrease after multiple repeating dialysis cycles, which will certainly decrease the overall fluorescence intensity of the hybrid microgels because only those QDs remained in the interior of microgels will contribute to the PL intensity of hybrid microgels. Because the CdS QDs may act as crosslinking points, the escape of the QDs could also lead to a relative loose network that causes a larger swelling degree. For those QDs remained in the interior of the microgels (possible crosslinking points), the larger swelling degree of microgels will not only generate a larger degree change of local refractive index around the QDs, but also stretch more on the polymer–QD interface, resulting in a larger quenching in PL intensity. In contrast, the PL quenching and recovery cycles of the p(NIPAM–AAm–FPBA)–CdS_{is} hybrid microgels are fully reproducible. The PL intensity can return to above 95% of its original basal value upon the removal of glucose even after five cycles and the peak shape was unchanged. These results demonstrate that the structure of the p(NIPAM–AAm–FPBA)–CdS_{is} hybrid microgels with in situ immobilized CdS QDs was very stable during the swelling/deswelling process, which attest to the photostability and general robustness of this sensor system.

3.3. *Interference of* L-*lactate*

Boronic acid can also bind other *cis*-diol metabolites that may potentially interfere with eventual determination of glucose in a physiological sample. The concentration of pyruvate, galactose and fructose in blood is <0.1 mM (Landon et al., 1962; James et al., 1994), thus it is unlikely that these compounds will interfere significantly with the glucose reading. However, L-lactate, an α-hydroxy acid, is presented in significantly higher concentrations. It is probable that the lactate would be the primary interferent if the present sensors were used on a physiological sample. Indeed, we found that the hybrid microgels are responsive to lactate (Fig. S-3) as lactate also possesses a suitable *cis*-diol structure (Sartain et al., 2008). The PL intensity can be quenched about 15% and 10%, respectively, for the p(NIPAM–AAm–FPBA)–CdS_{is} and p(NIPAM–AAm–FPBA)–CdS_{ab} hybrid microgels in the presence of 25 mM lactate, at which the microgels nearly reach a maximum swelling. In contrast, the PL intensity of the same hybrid microgels can be quenched as high as 65% and 56%, respectively, in the presence of 25 mM glucose (Fig. 3C). It is clear that our hybrid microgels demonstrate a high optical selectivity in response to glucose over lactate. The position of the hydroxyl groups on different sugars affects the affinity to boronic acids and thus the response of the sensor, as binding is known to occur only with suitably configured *cis*-diols (Davis and Wareham, 1999; Lee et al., 2004; Sartain et al., 2008). Boronic acids preferentially bind glucose in the tetrahedral form and lactate in the trigonal form (Kabilan et al., 2005; Yang et al., 2006). Although the binding of glucose to PBA in tetrahedral form is only observed at pH above 8, Lowe's group reported that the FPBA-modified polymer holographic films displayed the selectivity for glucose over lactate (Kabilan et al., 2005). They suggested that the incorporation of FPBA into the polymer film could lower the pH at which the tetrahedral form appears. We speculate that the selectivity of our hybrid microgel sensors to glucose over lactate at physiological pH is possibly attributed to the stabilization of the boronate ester by the adjacent amide groups presented in the gel network chains through the Lewis acid–base interactions between the electron-poor boron atom in FPBA groups and the electron-rich nitrogen atom in amide groups (Scheme S-3). A similar selective glucose-sensing behavior at physiological pH was also observed in the poly(vinyl alcohol)/amine-containing systems (Hisamitsu et al., 1997). Moreover, there may be an enhanced solvolysis of the PBA groups in the presence of amide groups. In a protic media, solvent insertion of the boronate, which affords hydrogen-bonded zwitterionic species, is the dominant reason for the formation of tetrahedral form in o-(*N*,*N*-dialkylaminomethyl) arylboronates (Zhu et al., 2006).

Fig. 4 shows the impact of a range of lactate concentrations (2-20 mM) on the glucose sensing response of the p(NIPAM–AAm–FPBA)–CdS_{is} hybrid microgels. The competitive binding of lactate to boronic acids in the hybrid microgels reduces the glucose binding degree, thus decreases the sensitivity of the hybrid microgels in response to glucose. The deviation become more pronounced at high lactate concentrations (e.g., 20 mM). However, since the

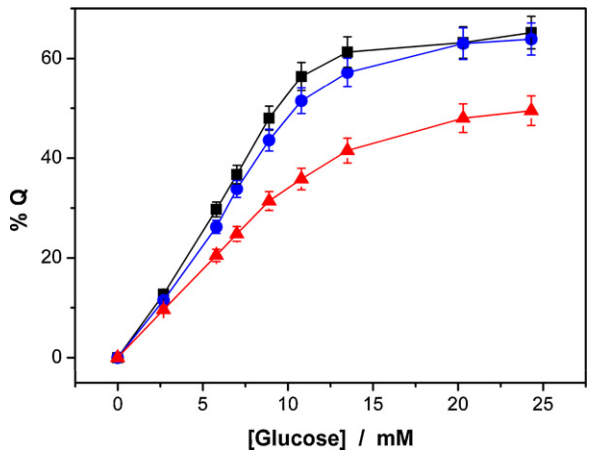

Fig. 4. Glucose response of the p(NIPAM–AAm–FPBA)–CdS_{is} hybrid microgels in the presence of L-lactate at different concentrations (■: 0 mM; ●: 2.0 mM; ▲: 20.0 mM).

lactate concentration in a resting healthy adult lies approximately 0.36–0.75 mM (Burtis and Ashwood, 1999), the data in Fig. 4 indicate that our hybrid microgel glucose sensors should be free from the significant interferences of lactate, as there was only about 1–3% change in glucose-induced PL quenching in the presence of 2.0 mM lactate.

3.4. Interference of human serum albumin

Human serum albumin, the most abundant protein in human serum, is known to undergo a slow non-enzymatic glycation (Burtis and Ashwood, 1999). The glycation eventually can result in the formation of Advanced Glycosylation End Products (AGE), which result in abnormal biological effects (Pertyńska-Marczewska et al., 2009). Under certain pathologic conditions, e.g., oxidative stress due to hyperglycemia in patients with diabetes, AGE formation can be increased beyond normal levels. AGEs are now known to play a role as proinflammatory mediators in gestational diabetes as well (Gugliucci, 2000). To examine the impact of HSA on the optical glucose response of our hybrid microgels, we have characterized the glucose-induced PL quenching of the hybrid microgels in the presence of HSA at a concentration of 44 g/L that is typically found in serum (Fig. S-4) (Burtis and Ashwood, 1999).

Fig. 5 shows that the presence of 44 g/L HSA in the PBS dispersion medium of hybrid microgels increases the glucose-induced PL quenching, resulting in a plausibly slight increase in the glucose-responsive sensitivity. At low glucose concentrations ($\leq$13.5 mM), the HSA-induced increase in the glucose-responsive PL quenching is not significant (<5%). At higher glucose concentrations (>13.5 mM), however, the glucose-responsive PL quenching does not reach a plateau as it does in the absence of HSA, which can be attributed to the competitive binding of HSA to boronic acids. The overall increase in the glucose-responsive PL quenching is related to the changes in the swelling ratio of the hybrid microgels upon the HSA binding. The boronic acid moieties on the microgels are capable of binding HSA, even in its nonglycosylated state (Muscatello et al., 2009). As the HSA is a relatively large molecule compared to glucose, the initial binding of HSA within the microgel hinders the accessibility of boronic acid sites that would normally be accessible to glucose. The addition of glucose and subsequent glycosylation of the HSA protein can further elevate its role as a competitive binder.

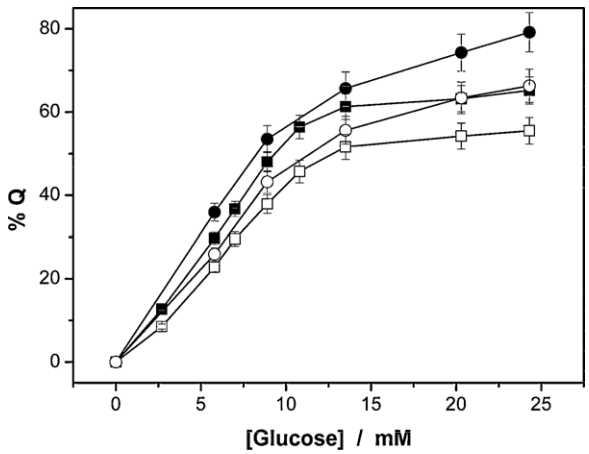

Fig. 5. Glucose response of the hybrid microgels in the absence and presence of 44 g/L HSA [p(NIPAM–AAm–FPBA)–CdS_{is}: ■—0 g/L, ●—44 g/L; p(NIPAM–AAm–FPBA)–CdS_{ab}: □—0 g/L, ○—44 g/L].

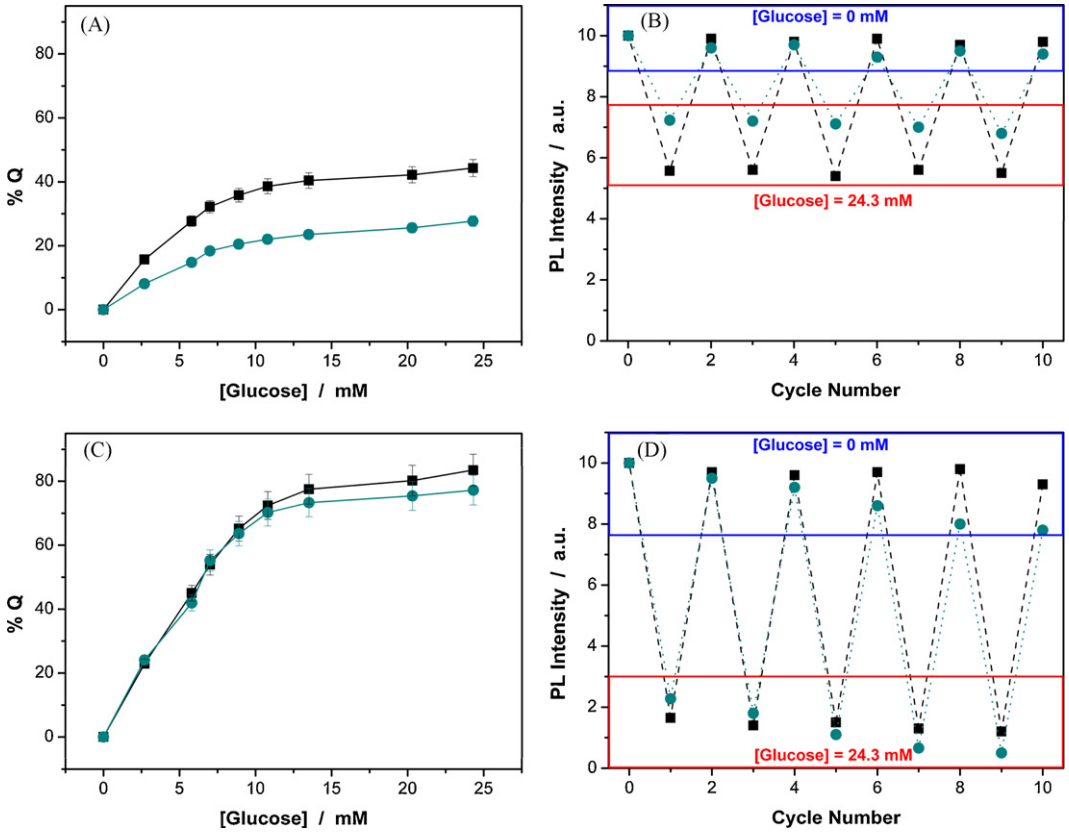

Fig. 6. Glucose-responsive PL properties (PBS, pH 7.38) of the p(NIPAM–AAm–FPBA)–CdS_{is} (■) and p(NIPAM–AAm–FPBA)–CdS_{ab} (●) hybrid microgels with crosslinking ratio of (A) 6.8% and (B) 3.2%, respectively. The PL quenching and recovery cycles upon repeated glucose addition/dialysis removal were also presented for the corresponding hybrid microgels with different crosslinking degree ((C) 6.8%; (D) 3.2%).

The binding of larger HSA to the FPBA sites of hybrid microgels can cause a larger swelling degree, thus lead to a larger PL quenching. This is similar to the competitive binding phenomenon observed in Asher's glucose sensors (Muscatello et al., 2009).

3.5. Tunable glucose-responsive sensitivity of hybrid microgels with variable crosslinking degree

We have demonstrated that both the p(NIPAM–AAm–FPBA)–CdS_{is} and the p(NIPAM–AAm–FPBA)–CdS_{ab} hybrid microgels with 4.3 mol% crosslinker display high sensitivity and selectivity for glucose. However, the optical response of the latter is not fully reversible after repeated swelling/deswelling cycles due to the gradual release of QDs from the microgels. These results reveal that the structure of the hybrid microgels should be one important factor to optimize the sensor property. To look into the structure–property relationship of the hybrid microgel sensing system, we prepared two additional p(NIPAM–AAm–FPBA) microgels with different crosslinking degrees. The variety of crosslinking degree will not only change the maximum swelling degree (or mesh size) of the polymer networks, but also cause different morphologies of the hybrid microgels after immobilization of CdS QDs (Fig. S-5). The hybrid microgels with a higher crosslinking degree (6.8%) adopted a more compact structure and a core-shell morphology. In contrast, when a lightly crosslinked (3.2%) template microgel is used to in situ grow or upload the CdS QDs, the core-shell morphology becomes illegible, but more QDs can be anchored into the microgels.

Fig. 6A and B shows that the hybrid microgels with different crosslinking degrees exhibit a similar optical response to glucose level change but to different sensitivity (PL spectra in Fig. S-6) due to the different swelling degrees. In comparison with the PL quenching of 65% for the p(NIPAM–AAm–FPBA)–CdS_{is} hybrid microgels with crosslinking ratio of 4.3% (Fig. 3), a lower sensitivity of 44% PL quenching for the sample with a crosslinking ratio = 6.8% and a higher sensitivity of 83% PL quenching for the sample with a crosslinking ratio = 3.2% were, respectively, observed. Correspondingly, the detection limits are estimated to be about 0.9 and 0.3 mM for the high and low crosslinked hybrid microgel sensors. Although the optical sensitivity of the glucose sensors was decreased, the structure was more stable for the more heavily crosslinked hybrid microgels. At a high crosslinking ratio of 6.8%, the PL quenching and recovery processes were fully reproducible for both types of hybrid microgels after five repeated cycles of glucose addition/dialysis removal (Fig. 6C). In contrast, at a low crosslinking ratio of 3.2%, the PL intensity of the p(NIPAM–AAm–FPBA)–CdS_{ab} hybrid microgels gradually decreased upon the repeated glucose addition/dialysis removal processes due to the escape of the CdS QDs from the loose gel networks (Fig. 6D). Nevertheless, the PL quenching and recovery processes of the p(NIPAM–AAm–FPBA)–CdS_{is} hybrid microgels with CdS QDs in situ grown in the gel networks were nearly fully reproducible after five cycles of glucose addition/dialysis removal even at a low crosslinking ratio of 3.2%, which further demonstrate the excellent photostability and general robustness of this type of hybrid microgels as glucose sensors. We therefore present a series of novel hybrid microgels with not only the reversible glucose-sensitive PL property change but also the tunable glucose-sensitive degree of the PL property change through the structural manipulation of the hybrid microgels.

4. Conclusion

In summary, we have demonstrated the feasibility of using QDs immobilized in the well-designed glucose-responsive p(NIPAM–AAm–FPBA) microgels to monitor glucose level under physiological pH conditions. The *cis*-diol binding ligands of FPBA in the microgels can induce a glucose-sensitive swelling and shrinking of the polymer networks at physiological pH, which can modify the physicochemical environment of the QDs embedded in the microgels, converting biochemical signals into optical signals. The structure difference resulting from different synthetic methods or crosslinking degrees produce different loading amount of QDs and swelling degree of microgels, which can further control the glucose-responsive optical sensitivity of the hybrid microgels. The reversible glucose-responsive PL quenching and recovery, excellent photostability, and general robustness of the hybrid microgels make this sensing system ideal for continuous and reliable glucose monitoring under physiological conditions. Furthermore, the present hybrid microgels are nonconsumptive and easily miniaturizable, which make them suitable for use in small-volume systems and in a real time.

Acknowledgements

We gratefully acknowledge the financial support from the US Agency for International Development under the US-Pakistan Science and Technology Cooperative Program (PGA-P280422).

Appendix A. Supplementary data

Supplementary data associated with this article can be found, in the online version, at doi:10.1016/j.bios.2010.04.030.

References

Alexeev, V.L., Sharma, A.C., Goponenko, A.V., Das, S., Lednev, I.K., Wilcox, C.S., Finegold, D.N., Asher, S.A., 2003. Anal. Chem. 75, 2316.
Bardelang, D., Zaman, M.B., Moudrakovski, I.L., Pawsey, S., Margeson, J.C., Wang, D., Wu, X., Ripmeester, J.A., Ratcliffe, C.I., Yu, K., 2008. Adv. Mater. 20, 4517.
Burtis, C.A., Ashwood, E.R. (Eds.), 1999. Tietz Textbook of Clinical Chemistry, 3rd ed. W.B. Saunders, Philadelphia, PA.
Cordes, D.B., Gamsey, S., Singaram, B., 2006. Angew. Chem. Int. Ed. 45, 3829.
Davis, A.P., Wareham, R.S., 1999. Angew. Chem. Int. Ed. 38, 2979.
Freeman, R., Bahshi, L., Finder, T., Gill, R., Willner, I., 2009. Chem. Commun., 764.
Gill, R., Bahshi, L., Freeman, R., Willner, I., 2008. Angew. Chem. Int. Ed. 47, 1676.
Gugliucci, A., 2000. J. Am. Osteopathol. Assoc. 100, 621.
Hisamitsu, I., Kataoka, K., Okano, T., Sakurai, Y., 1997. Pharm. Res. 14, 289.
James, T.D., Sandanayake, K., Shinkai, S., 1994. Angew. Chem. Int. Ed. Engl. 33, 2207.
Kabilan, S., Marshall, A.J., Sartain, F.K., Lee, M.C., Hussain, A., Yang, X., Blyth, J., Karangu, N., James, K., Zeng, J., Smith, D., Domschke, A., Lowe, C.R., 2005. Biosens. Bioelectron. 20, 1602.
King, H., Aubert, R.E., Herman, W.H., 1998. Diabetes Care 9, 1414.
Landon, J., Fawcett, J.K., Wynn, V.J., 1962. Clin. Pathol. 15, 579.
Lee, M.C., Kabilan, S., Hussain, A., Yang, X., Blyth, J., Lowe, C.R., 2004. Anal. Chem. 76, 5748.
Li, X., Zhou, Y., Zheng, Z., Yue, X., Dai, Z., Liu, S., Tang, Z., 2009. Langmuir 25, 6580.
Li, Y., Tanaka, T., 1990. J. Chem. Phys. 92, 1365.
Lim, I.S., Chandrachud, U., Wang, L., Gal, S., Zhong, C.J., 2009. Acc. Chem. Res. 42, 798.
Liu, Y., Zhang, Y.J., Guan, Y., 2009. Chem. Commun., 1867.
Matz, K., Keresztes, K., Tatschl, C., Nowotny, M., Dachenhausenm, A., Brainin, M., Tuomilehto, J., 2006. Diabetes Care 29, 792.
McCowen, K.C., Malhotra, A., Bistrian, B.R., 2001. Crit. Care Clin. 17, 107.
Mulvaney, P., 1996. Langmuir 12, 788.
Muscatello, M.M., Stunja, L.E., Asher, S.A., 2009. Anal. Chem. 81, 4978.
Peng, B., Qin, Y., 2008. Anal. Chem. 80, 6137.
Pertyńska-Marczewska, M., Głowacka, E., Sobczak, M., Cypryk, K., Wilczyński, 2009. Am. J. Reprod. Immunol. 61, 175.
Pickup, J.C., Hussain, F., Evans, N.D., Rolinski, O.J., Birch, D.J.S., 2005. Biosens. Bioelectron. 20, 2555.
Reese, C.E., Mikhonin, A.V., Kamenjicki, M., Tikhonov, A., Asher, S.A., 2004. J. Am. Chem. Soc. 126, 1493.
Sartain, F.K., Yang, X., Lowe, C.R., 2008. Chem. Eur. J. 14, 4060.
Schmeltz, L.R., DeSanti, A.J., Thiyagarajan, V., Schmidt, K., O'Shea-Mahler, E., Johnson, D., Henske, J., McCarthy, P.M., Gleason, T.G., McGee, E.C., Molitch, M.E., 2007. Diabetes Care 30, 823.
Shoji, E., Freund, M.S., 2002. J. Am. Chem. Soc. 124, 12486.
Suri, J.T., Cordes, D.B., Cappuccio, F.E., Wessling, R.A., Singaram, B., 2003. Angew. Chem. Int. Ed. 42, 5857.
Tang, B., Cao, L., Xu, K., Zhou, L., Ge, J., Yu, L., 2008. Chem. Eur. J. 14, 3637.
Tierney, S., Hasle, B.M.H., Hjelme, D.R., Stokke, B.T., 2009. Anal. Chem. 81, 3630.
Van den Berghe, G., Wilmer, A., Hermans, G., Meersseman, W., Wouters, P.J., Milants, I., Van Wijngaerden, E., Bobbaers, H., Bouillon, R.N., 2006. Engl. J. Med. 354, 449.

Vantyghem, M.C., Haye, S., Balduyck, M., Hober, C., Degand, P.M., Lefebvre, J., 1999. Acta Diabetol. 36, 39.
Wang, J., Gan, D., El-Sayed, M.A., 2001. J. Am. Chem. Soc. 123, 11284.
Wu, W., Zhou, T., Zhou, S., 2009a. Chem. Commun., 4390.
Wu, W., Zhou, T., Aiello, M., Zhou, S., 2009b. Chem. Mater. 21, 4905.
Wuister, S.R., Donegá, C.M., Meijerink, A., 2004. J. Am. Chem. Soc. 126, 10397.
Xiong, Y.J., Siekkinen, A.R., Wang, J.G., Yin, Y.D., Kim, M.J., Xia, Y.N., 2007. J. Mater. Chem. 17, 2600.
Yang, W., He, H., Drueckhammer, D.G., 2001. Angew. Chem. Int. Ed. 40, 1714.
Yang, X., Lee, M.C., Sartain, F., Pan, X., Lowe, C.R., 2006. Chem. Eur. J. 12, 8491.
Yang, X., Pan, X., Blyth, J., Lowe, C.R., 2008. Biosens. Bioelectron. 23, 899.
Zhang, J., Xu, S., Kumacheva, E., 2004. J. Am. Chem. Soc. 126, 7908.
Zhang, Y., Guan, Y., Zhou, S., 2007. Biomacromolecules 8, 3842.
Zhu, L., Shabbir, S.H., Gray, M., Lynch, V.M., Sorey, S., Anslyn, E.V., 2006. J. Am. Chem. Soc. 128, 1222.